



**AALBORG UNIVERSITY**  
DENMARK

**Aalborg Universitet**

## **Power System Real-Time Emulation**

*A Practical Virtual Instrumentation to Complete Electric Power System Modeling*

Parizad, Ali; Mohamadian, Sobhan; Iranian, Mohammad Esmail; Guerrero, Josep M.

*Published in:*

IEEE Transactions on Industrial Informatics

*DOI (link to publication from Publisher):*

[10.1109/TII.2018.2837079](https://doi.org/10.1109/TII.2018.2837079)

*Publication date:*

2019

*Document Version*

Accepted author manuscript, peer reviewed version

[Link to publication from Aalborg University](#)

*Citation for published version (APA):*

Parizad, A., Mohamadian, S., Iranian, M. E., & Guerrero, J. M. (2019). Power System Real-Time Emulation: A Practical Virtual Instrumentation to Complete Electric Power System Modeling. *IEEE Transactions on Industrial Informatics*, 15(2), 889-900. Article 8360043. <https://doi.org/10.1109/TII.2018.2837079>

### **General rights**

Copyright and moral rights for the publications made accessible in the public portal are retained by the authors and/or other copyright owners and it is a condition of accessing publications that users recognise and abide by the legal requirements associated with these rights.

- Users may download and print one copy of any publication from the public portal for the purpose of private study or research.
- You may not further distribute the material or use it for any profit-making activity or commercial gain
- You may freely distribute the URL identifying the publication in the public portal -

### **Take down policy**

If you believe that this document breaches copyright please contact us at [vbn@aub.aau.dk](mailto:vbn@aub.aau.dk) providing details, and we will remove access to the work immediately and investigate your claim.

# Power System Real-Time Emulation: A Practical Virtual Instrumentation to Complete Electric Power System Modelling

Ali Parizad, *Graduate Student Member, IEEE*, Sobhan Mohamadian, Mohamad Esmaeil Iranian, and Josep M. Guerrero, *Fellow, IEEE*

**Abstract**— **Hardware-in-the-loop (HIL) simulation is a technique that is being used increasingly in the development and test of complex systems. Real-world testing of an intricate system in a field like power plant can be challenging, time-consuming, expensive, and hazardous. HIL emulators allow engineers to test devices thoroughly and efficiently in a virtual environment with high reliability and minimum risk of defect. In this paper, the complete electric power system (including generator, turbine-governor, excitation system, transmission lines, transformer, external grid and related loads) is implemented in MATLAB/Simulink environment. Different virtual instrument (VI) pages are modeled in the graphical programming language of LabVIEW which enable fast and reliable measurement functions such as data acquisition, archiving, real-time graphical display and processing. The interaction between MATLAB and LabVIEW is accomplished by generating a Phar Lap ETS Targets \*.dll file which enables the two software to exchange real-time data. Also, a real 1518 kW excitation system is considered as a test case for introduced HIL system. This equipment is connected to LabVIEW software through a National Instrument PXI technology. Different scenarios (electrical frequency/active power change, voltage step response and etc.) are simulated in the designed Power System Emulator (PSE). The validity of implemented model for excitation system is verified by finding good matching between MATLAB and HIL simulation results.**

**Index Terms**—**hardware-in-the-loop (HIL), LabVIEW, power system emulator (PSE), real-time simulation, virtual instrument.**

## I. INTRODUCTION

**O**FFLINE simulation of the electric power systems and their control in software tools such as MATLAB/Simulink, PSpice, PSIM, DIgSILENT, etc., is one of the most prevalent methods to verify the design considerations of such systems. It is possible to evaluate the performance of the complex designed system under different working conditions by offline simulation before it enters the manufacturing stage. Since the mathematical model of electric power system devices

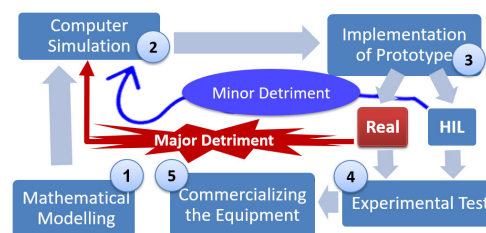


Fig. 1. HIL and real-time system's role in test of equipment

such as electrical machines and transformers includes differential equations, the running time of their model in the above-mentioned environments is significant compared to the real time [1], [2]. Furthermore, the offline nature of simulations yields unwanted differences with respect to the experiments carried out in real time [3]. Hence, offline simulation results are not 100% reliable.

Real-time digital simulation or the so-called hardware-in-the-loop (HIL) simulation is a reliable approach which is widely used to examine the electric power systems and their control methodologies [4], [5]. HIL simulation combines the advantages of both offline simulation and experiments on the real set-up. Compared to offline simulation, HIL simulation results are more realistic and closer to the experimental ones [6], [7].

As shown in Fig. 1, it is necessary to verify electric power equipment functionality prior to commercializing the equipment and before going through mass production. In general, after mathematical modeling and computer simulation, a prototype is implemented to go under some experimental tests. In this way, any fault due to miscalculation or implementation may cause major detriment to the equipment and related network. To prevent such a dilemma, HIL technology has been proposed. Applying HIL technology and real-time systems provides the required environmental reality via simulation so that test procedure of the equipment does not affect anything beyond the equipment itself. This replacement would decrease the risk and detriment of consequential damage. In other words, HIL technology not only expedites the test procedure but also reduces the costs and makes the whole procedure much more reliable and flexible.

HIL simulation has two categories: (1) Controller HIL (CHIL), and (2) power HIL (PHIL) simulations. In the first type, i.e., CHIL, real controller is tested while the other elements of the electric power system are modeled in the

A. Parizad is with the MAPNA Electric and Control Eng. and Manuf. Co. (MECO), Iran; (e-mail: ali.parizad@ieee.org).

S. Mohamadian is with the School of Engineering, Damghan University, Damghan, Iran (e-mail: s.mohamadian@du.ac.ir).

M.E. Iranian is with the MAPNA Electric and Control Eng. and Manuf. Co. (MECO), Iran (e-mail: iranian@mapnaec.com)

J.M. Guerrero is with the Department of Energy Technology, Aalborg University, 9220 Aalborg East, Denmark (joz@et.aau.dk).

Corresponding Author: A. Parizad (ali.parizad@ieee.org).

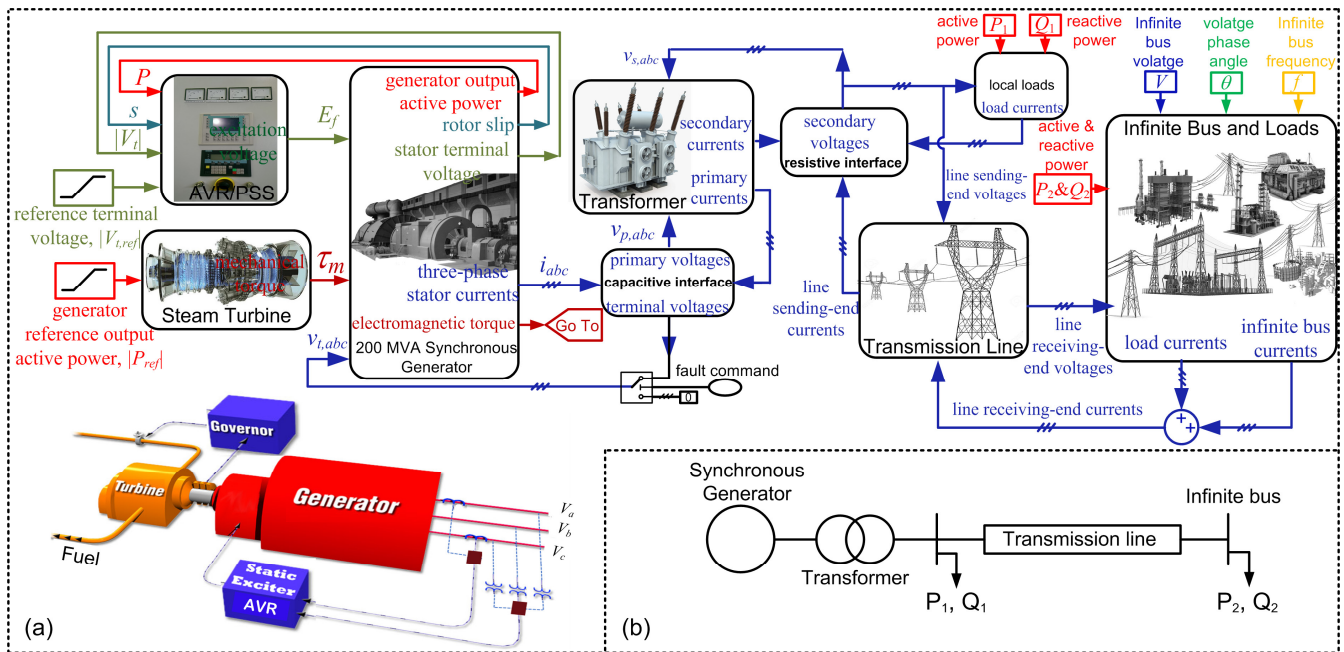


Fig. 2. (a) Overall scheme of the implemented MATLAB/Simulink model of the complete power system and (b) single-line diagram of the electrical part.

software. Various applications of CHIL simulations are available in literature to examine the control units of electric power equipment [8]-[15]. On the other hand in PHIL simulation, a part of the power circuit is external to the simulator where a power amplifier is needed to transfer the real power to the hardware [7], [16]-[22]. PHIL simulation gives the advantage of testing a part of power circuit before the other parts come into the manufacturing procedure.

Besides providing a realistic examination tool for electric power systems, HIL is also very fruitful for educational purposes specifically for undergraduate students. For instance, implementing a complex electric power network consisting of synchronous generator, steam turbine, transformers, transmission lines, load and infinite bus in which the synchronous generator is connected to the model of a real excitation system is literally troublesome for an undergraduate student to conceive the principles of the network operation and analyze the actual performance of the exciter and its inbuilt function blocks such as power system stabilizer (PSS). As an illustration, students need to understand the changes in the outputs of PSS, or rotor frequency or temperature of turbine inlet steam when a three-phase short-circuit occurs in the transmission line without the need to know about the synchronous machine differential equations in the  $q-d$  reference frame. Instead, a real-time emulator with virtually implemented instrument including a software tool like MATLAB/Simulink which represents the overall system model and a user-friendly interface such as LabVIEW can help the students to gain a profound understanding of the power system operation under several scenarios while preserving their time and safety compared to the offline simulation and experimental activities, respectively. Similar HIL structures using LabVIEW have been reported in the literature for the educational purposes [23]-[26] and implementing measuring and testing apparatuses [27]-[31].

LabVIEW is an advanced high-level programming and

graphical language which creates a flexible HIL simulation structure for the operator in order to optimize and increase the efficacy of the program [32]-[35].

In this study, the above-mentioned complete electrical and mechanical components in power network are modeled in MATLAB/Simulink environment. LabVIEW and related modules such simulation interface toolkits are utilized for implementing codes and also as a graphical interface between real excitation cubicle, simulation software, and the operator (Human/Machine Interface (HMI)).

In this paper, the procedure to build a virtual instrument as a power system emulator (PSE) is explained in detail. Consistent to this issue, dynamic models of turbine, generator, power transformer, line, load, and an external grid for a real excitation system are implemented. Accordingly, the paper is organized as follows. In Section II, tips on creating a unified MATLAB/Simulink model of the entire power network are highlighted. Section III is dedicated to a thorough description on constructing a real-time simulator of the electric power system. Requirements for interfacing the computer model with the external hardware via LabVIEW are explained and necessary guidelines for connections and settings of the hardware are emphasized. A comprehensive set of scenarios for simulation and experimental studies are conducted in Section IV to verify the proposed PSE. Finally, conclusions are drawn in Section V.

## II. IMPLEMENTED MODELS IN MATLAB/SIMULINK

As a first step of the PSE construction process, complete model of an electric power system is established in MATLAB/Simulink software tool. As shown in Fig. 2, the implemented model of the overall system consists of several subsystems representing the model of every single constituent of an electric power system. Generally, the system can be studied in two subsections as follows:

### A. Electrical

As a rule of thumb in modeling the electrical components, it is better to set the differential equations of each subsystem in such a way so that the outputs are an integral of the inputs because the integrator is less susceptible to high-frequency noise than differentiator [36]. Hence, due to the inductive nature of most power system components such as synchronous generator and transformer, voltages and currents are better to be inputs and outputs, respectively. As a result, an interface is needed to turn the outputs of the synchronous generator, i.e., three-phase currents, into the suitable inputs, i.e., voltages, for the transformer model (see Fig. 2(a)). The interface can be a three-phase capacitance or resistance with an impedance much higher (10 times or higher) than the system base impedance [36].

In the following, a brief description of each electrical subsystem model is presented.

#### 1) Synchronous generator

Synchronous generator model consists of a set of six electrical differential equations (stator three-phase and rotor excitation and two damper circuits along  $q$  and  $d$  axes) to obtain electro-magnetic torque and three-phase currents from stator three-phase and rotor (excitation and damper) circuits input voltages. The model also consists of one electro-mechanical differential equation to obtain rotor angle from the input load and electro-magnetic torques. The electrical equations, i.e., Park equations, are implemented in the rotor  $q$ - $d$  reference frame as follows [36], [37]:

$$\frac{d}{dt} \mathbf{i}_{qd} = \mathbf{L}_{qd}^{-1} \left[ \mathbf{v}_{qd} - (\mathbf{R} + \omega \mathbf{J} \mathbf{L}_{qd}) \mathbf{i}_{qd} \right], \quad (1)$$

$$\boldsymbol{\lambda}_{qd} = \mathbf{L}_{qd} \mathbf{i}_{qd},$$

with

$$\mathbf{v}_{qd} = (v_{qs}, v_{ds}, v_{0s}, 0, 0, v'_f)^t, \quad \mathbf{i}_{qd} = (i_{qs}, i_{ds}, i_{0s}, i'_{kq}, i'_{kd}, i'_f)^t,$$

$$\boldsymbol{\lambda}_{qd} = (\lambda_{qs}, \lambda_{ds}, \lambda_{0s}, \lambda'_{kq}, \lambda'_{kd}, \lambda'_f)^t, \quad \mathbf{J} = \begin{pmatrix} 0 & 1 & \mathbf{0}_{1 \times 4} \\ -1 & 0 & \mathbf{0}_{1 \times 4} \\ \mathbf{0}_{4 \times 1} & \mathbf{0}_{4 \times 1} & \mathbf{0}_{4 \times 4} \end{pmatrix} \quad (2)$$

$$\mathbf{L}_{qd} = \begin{pmatrix} L_{ls} + L_{mq} & 0 & 0 & L_{mq} & 0 & 0 \\ 0 & L_{ls} + L_{md} & 0 & 0 & L_{md} & L_{md} \\ 0 & 0 & L_{ls} & 0 & 0 & 0 \\ L_{mq} & 0 & 0 & L'_{kq} + L_{mq} & 0 & 0 \\ 0 & L_{md} & 0 & 0 & L'_{kd} + L_{md} & L_{md} \\ 0 & L_{md} & 0 & 0 & L_{md} & L'_{lf} + L_{md} \end{pmatrix}$$

In the above equations,  $u_{qs}$ ,  $u_{ds}$ ,  $u_{0s}$  are the stator transformed quantities to the rotor reference frame.  $u'_{kq}$ ,  $u'_{kd}$ ,  $u'_f$  are the rotor  $kq$  and  $kd$  damper windings and excitation quantities, respectively. Parameter  $u$  can be either voltage,  $v$ , current,  $i$ , or flux linkage,  $\lambda$ . Furthermore,  $L_{ls}$ ,  $L'_{kq}$ ,  $L'_{kd}$ ,  $L'_{lf}$  are the leakage inductances of the stator  $qd0$  and rotor  $kq$ ,  $kd$ , and field windings, respectively.  $L_{mq}$  and  $L_{md}$  are magnetizing inductances along  $q$  and  $d$  axes, respectively. Finally,  $\mathbf{R}$  is the  $6 \times 6$  diagonal matrix representing different winding resistances.

Synchronous machine rotor revolution,  $\omega$  in (1), is the output of the electro-mechanical equation:

$$\tau_{em} - \tau_m = J_s \frac{d\omega}{dt}, \quad (3)$$

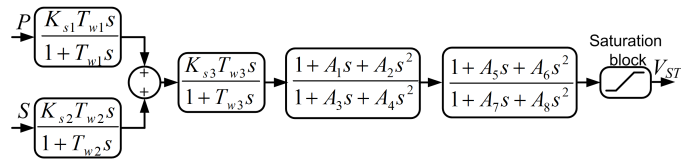


Fig. 3. Implemented PSS model.

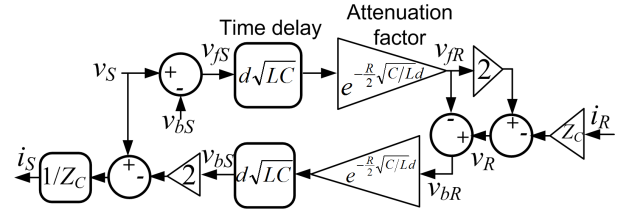


Fig. 4. Distributed line model.

where,  $\tau_{em}$  and  $\tau_m$  are the generator electro-magnetic torque and gas turbine mechanical torque, respectively.  $J_s$  is the inertia of the machine shaft.  $\tau_{em}$  in (3) is calculated as follows:

$$\tau_{em} = \frac{3p}{2} \mathbf{i}'_{qd} \mathbf{J} \mathbf{L}_{qd} \mathbf{i}_{qd}, \quad (4)$$

in which,  $p$  is the machine pole numbers.

A capacitive interface generates machine stator three-phase voltages through the three-phase stator and primary currents of the machine and transformer models as shown in Fig. 2 (a). These voltages are then fed back as the generator model inputs (Eq. (1)). Excitation voltage ( $v'_f$  in (1)) is applied from the AVR/PSS subsystem output. As shown in Fig. 2(a), the inputs to the PSS model are the generator output electric power,  $P$ , and rotor slip,  $S$ . For validation purposes in the experimental activities, a practical model from SIEMENS Corporation is implemented as AVR/PSS. In Fig. 3, a block diagram of the SIEMENS PSS model, i.e., PSS3B, is shown. In this figure,  $s$  is the Laplace operator. Model output, i.e.,  $V_{ST}$ , is then compared to the reference value to produce the excitation voltage,  $E_f$ , through the field circuit controller.

#### 2) Three-phase transformer

Similar to the generator, the inputs of the transformer model are primary (low-voltage) and secondary (high-voltage) voltages in which the former are identical to the generator stator three-phase voltages and the latter are the outputs of a resistive interface that works with the output currents of the transformer secondary windings, local loads, and the sending end of the distributed line model (Fig. 2(a)). Three-phase primary and secondary voltages,  $v_1$  and  $v'_2$ , are utilized to obtain three-phase primary and secondary currents from two sets of differential equations representing each phase of transformer model [36]:

$$\psi_1 = \int \left[ v_1 - r_1 \left( \frac{\psi_1 - \psi_m}{L_{l1}} \right) \right] dt; \quad \psi'_2 = \int \left[ v'_2 - r'_2 \left( \frac{\psi'_2 - \psi_m}{L'_{l2}} \right) \right] dt. \quad (5)$$

In the above equation,  $\psi_1$  and  $\psi'_2$  are the primary and secondary windings linkage fluxes and  $\psi_m$  is the mutual flux. ( $r_1$ ,  $r'_2$ ) and ( $L_{l1}$ ,  $L'_{l2}$ ) are the primary and secondary windings resistances and leakage inductances, respectively. Note that the secondary quantities are referred to the primary side.

$\psi_m$  and primary and secondary currents,  $i_1$  and  $i'_2$ , are calculated as follows:

$$i_1 = \frac{\psi_1 - \psi_m}{L_{l1}}; \quad i'_2 = \frac{\psi'_2 - \psi_m}{L'_{l2}}; \quad \psi_m = L_M \left( \frac{\psi_1}{L_{l1}} + \frac{\psi'_2}{L'_{l2}} \right); \quad (6)$$



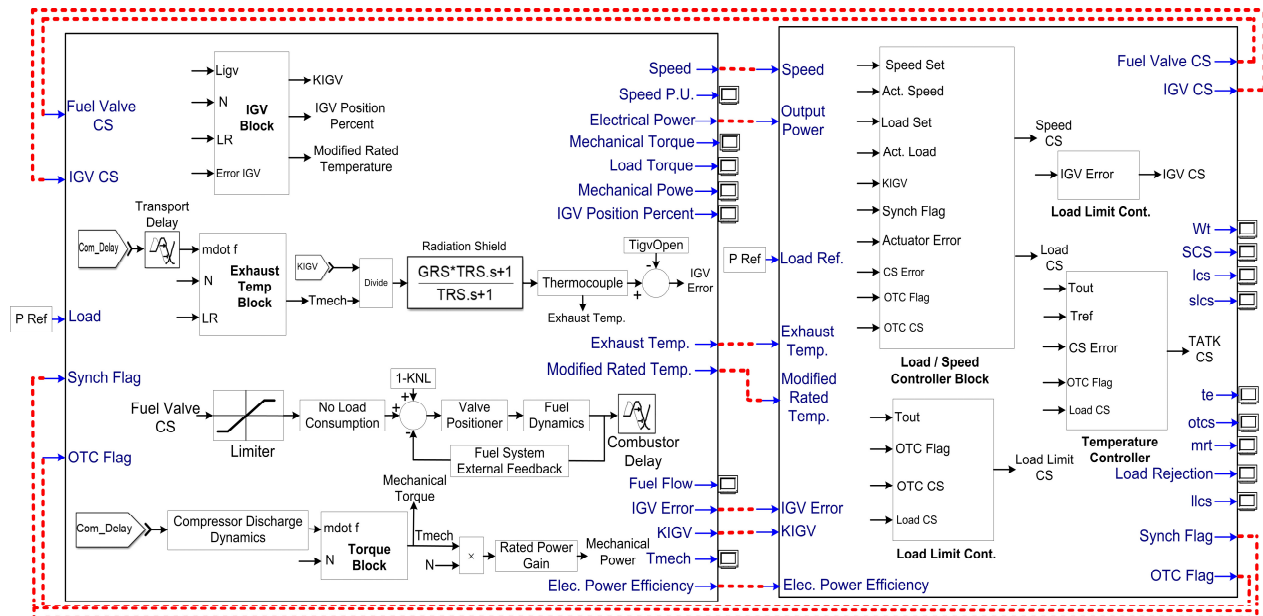


Fig. 5. Overall schematic block diagram of turbine-governor model in MATLAB Simulink.

where,  $1/L_M = 1/L_{m1} + 1/L_{l1} + 1/L'_{l2}$  with  $L_{m1}$  being the primary-referred magnetizing inductance.

### 3) Transmission line

A power plant is connected to an infinite bus and electrical loads via transmission lines. A distributed line model based on Bewley lattice diagram [36] is considered to accurately model the transmission line irrespective of its length,  $d$ . The model is shown in Fig. 4. As can be seen in Fig. 2 and Fig. 4, model inputs (outputs) are the sending-end (receiving-end) three-phase voltages and the receiving-end (sending-end) three-phase currents. In other words,  $v_S, i_R$  are the inputs and  $v_R, i_S$  are the outputs of each phase. Based on this model, the voltage and current in every position of line are composed of forward and feedback waves, i.e.,  $(v_f, v_b)$  and  $(i_f, i_b)$ . Hence,

$$v_S = v_{fS} + v_{bS} = Z_C i_{fS} - Z_C i_{bS}; \quad v_R = v_{fR} + v_{bR} = Z_C i_{fR} - Z_C i_{bR} \quad (7)$$

where,  $Z_C$  is the characteristic impedance of the line and is a function of line per meter series inductance,  $L$ , and shunt capacitance,  $C$ , as  $Z_C = \sqrt{L/C}$ .

As shown in Fig. 4, backward and forward components of the sending- and receiving-end voltages, i.e.,  $v_{bS}$  and  $v_{fR}$ , respectively, are extracted via applying attenuation factor and time delay to their forward and backward components. Also, (8) can be derived according to (7) as

$$v_S = Z_C (i_S - i_{bS}) - Z_C i_{bS} = Z_C i_S + 2v_{bS}; \quad v_R = 2v_{fR} - Z_C i_R \quad (8)$$

### 4) Infinite bus and loads

An infinite bus is modeled so that the operator can set its voltage amplitude and frequency. Loads are realized according to their active,  $P_2$ , or reactive powers,  $Q_2$ . Load resistance, inductance or capacitance can be extracted according to active and reactive powers. Then, differential equations are solved based on inputs (voltages) to calculate the outputs (currents).

### B. Mechanical

Different models have been developed in literature in order to represent the gas turbine behavior. In this paper, the expanded Rowen's model of a heavy-duty single-axis gas turbine is used as the reference model [38]. Fig. 5 shows the

overall schematic block diagram of turbine-governor model in MATLAB/Simulink. The gas turbine operates in a simple cycle with no heat recovery in which the cycle consists of a 16-stage compressor with a pressure ratio of 1:11.75, two vertical combustion chambers, and 4-stage power turbines [39]-[41]. Also, constant speed is fixed between 95%–107% of the rated speed. The single-shaft gas turbine is represented along with the control and fuel systems. Control system of the gas turbine has three loops: speed, temperature, and acceleration control loops. These three control functions are all inputs into a minimum selector. The output of the selector shows the least fuel control action among the three control actions. The speed control loop conducts directly the governor and can be operated in the standard droop configuration or in isochronous mode. The temperature control loop maintains the gas turbine output temperature within its constraints. Exhaust temperature is measured using a series of thermocouples incorporating radiation shields. In order to prevent the over-speeding of the generator in the event of a sudden loss of load, an acceleration control loop is simulated in the model and applied to the minimum value selector as the third input.

Also, the model of inlet guide vanes (IGVs) controller is taken into account which manages the outlet temperature of the turbine. Considering V94.2 SIEMENS turbine-governor parameters, this model has been used to study the governor and the gas turbine operation. A system of seven differential equations with three inputs and seven state-space variables is solved to represent the behavior of the gas turbine. State-space variables are: fuel valve angle ( $\theta$ ), fuel flow ( $q_f$ ), air flow ( $q$ ), speed ( $N$ ), temperature inside the radiation shield of the thermocouple ( $T_{sh}$ ), measured temperature ( $T$ ), and the outlet of the IGV ( $L_{IGV}$ ). Inputs are: (1) control valve signal ( $u_1$ ) which its maximum and minimum constraints are limited to high and low saturation quantities of fuel valve, respectively, (2) IGV signal that is saturated by its constraints  $minIGV$  and  $maxIGV$ , and (3) synchronous machine electro-magnetic torque ( $\tau_{em}$ ). The state-space equations are as follows:

$$\begin{aligned}
 \frac{d}{dt} \theta &= -\frac{1}{b} \theta + \frac{KNL + (1 - KNL)Nu_1}{b} \\
 \frac{d}{dt} q_f &= \frac{\theta - q_f}{T_{FS}} \\
 \frac{d}{dt} q &= \frac{e^{-T_{CR} s} q_f - q}{T_{CD}} \\
 \frac{d}{dt} N &= \frac{1}{J} (\tau_m - \tau_{em}) \\
 \left\{ \begin{aligned}
 \frac{d}{dt} T_{sh} &= \frac{T_m(1 - G_{RS}) - T_{sh}k_{IGV} - G_{RS}k_{IGV}}{T_{RS}k_{IGV}(1 - G_{RS})} \\
 \frac{d}{dt} T &= \frac{T_{sh} - T}{T_T} \\
 \frac{d}{dt} L_{IGV} &= \frac{u_2 - L_{IGV}}{T_{IGV}}
 \end{aligned} \right. \quad (9)
 \end{aligned}$$

where,  $b$ ,  $KNL$ ,  $k_{IGV}$ , and  $G_{RS}$  represent valve positioner time constant, minimum fuel flow to maintain flame, IGV effect on the output temperature, and radiation shield parameter, respectively. Also,  $T_{FS}$ ,  $T_{CR}$ ,  $T_{CD}$ ,  $T_{RS}$ ,  $T_T$ ,  $T_{IGV}$  are the time constants of the fuel system, combustion system, compressor discharge lag, radiation shield, thermocouple, and IGV, respectively.

Turbine output mechanical torque,  $\tau_m$ , and output temperature,  $T_m$ , in (9) are obtained via the following equations:

$$\tau_m = A + Bq + C(1 - N), \quad (10)$$

$$T_m = T_R + D_1(e^{-T_{CR} s} e^{-T_{TD} s} q_f) + D_2 + E(1 - N), \quad (11)$$

where,  $A$ ,  $B$ , and  $C$  in (10) are constants of the gas turbine torque equation.  $D_1$ ,  $D_2$ ,  $E$  in (11) are constants of the gas turbine outlet temperature and  $T_R$  is the exhaust gas rated temperature. Fixed-step ode5 (Dormand-Prince) is used as the simulation solver. A brief description of the HIL computation unit is provided in Section III.

### III. REAL-TIME IMPLEMENTATION

As mentioned in Section II, different power system constituents are modeled and simulated in MATLAB/Simulink. In order to connect MATLAB models with LabVIEW, it is necessary to build a file with \*.dll format from Simulink and import it into the written program in LabVIEW environment. This dynamic library is generated by NI simulation interface toolkit (SIT) [42]. This program and related subprograms provide a way to create a LabVIEW user-friendly interface which helps to communicate with a Simulink model, manipulate the model parameters and view the output data of the Simulink model. As shown in Fig. 6, the LabVIEW program should be deployed in real-time system (RTS). In this project, a National-Instrument PXIe-8133 [43] and related devices (Fig. 6–box 2) serve as the real-time implementation of the power system. For the sake of experimental verification of the proposed PSE, a real excitation system is utilized to make a HIL emulator as shown in Fig. 6. For the communication purposes between excitation control system and the computer, the PXI provides I/O modules with accuracy and time delay characteristics as in the following: (1) The analog output (AO)

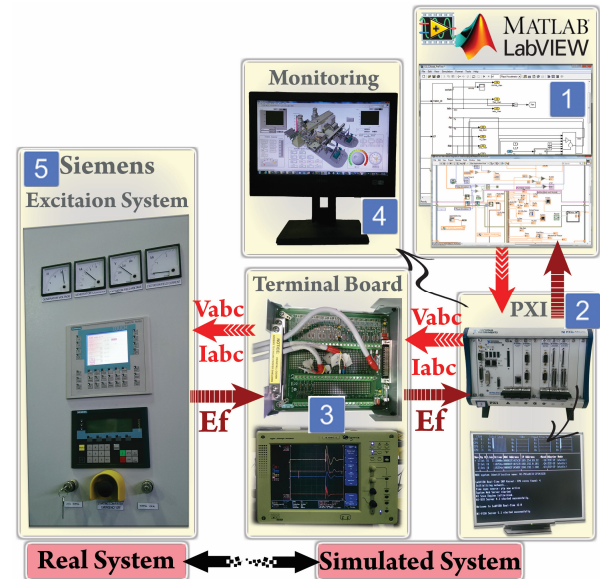


Fig. 6. Overall scheme of the simulated and real-time systems

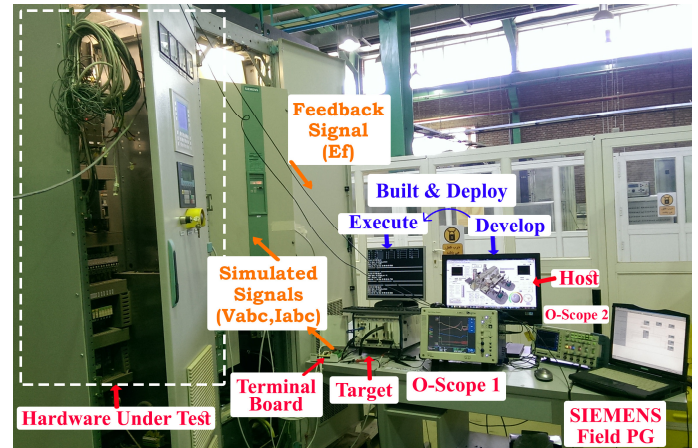


Fig. 7. Hardware setup for HIL simulation of the excitation system and related I/O connections

module is used to send three-phase voltage and current signals from PXI-7833R [43] to the excitation system. It is adopted for the module with a sampling rate of 1 MHz and a 16-bit resolution. (2) The analog input (AI) module is used to receive excitation voltage ( $E_f$ ) signal from the excitation system through the terminal board shown in Fig. 6 (NI-SCB-68). PXI-7833R is adopted for the module with a sampling rate of 200 kHz and a 16-bit resolution. The loop, in the simulated model, is closed by feeding the excitation voltage signal back into the RTS in which the step time of the calculations is 300 microseconds. Hardware setup for HIL simulation of the excitation system and related I/O connections is shown in Fig. 7.

It should be mentioned that the ordinary real-time implementation of a limited electric power system equipment (generator, excitation system, and infinite bus) has been presented in [44] utilizing a single PCI 7831R plus an Advantech PC (PC based system) in which the operating system (OS) is Phar Lap 13.1. Also, in [45] a simple configuration of power system using a commercial PC, a PCI card and Ardence RTX to form a real-time subsystem (RTSS) has been implemented. In the latter study, all of the models and even the



solver have been developed inside the LabVIEW missing the advantages of utilizing MATLAB/Simulink models implementation. On the contrary to the mentioned studies, as shown in Fig. 7, a professional and comprehensive test rig with flexible and expandable structure has been developed in this paper with the use of high technology National Instrument equipment linked to MATLAB and LabVIEW. The system can be much more professionally configured as discussed in the following.

#### IV. CONFIGURATION AND SETTINGS

As mentioned in the previous section, PXI-7833R is used to interchange voltages and currents signals between software and related terminal points in the excitation cabinet. NI-SCB-68 terminal board (Fig. 6–box 3) [43] is used to transfer signals between RTS and SIEMENS board in the external system (i.e., excitation system in Fig. 6–box 5). Wiring diagram between terminal board and SIEMENS board is established according to SIEMENS datasheet.

FPGA, PXIe-8133, and PC are considered as three distinct environments in order to implement real-time functionality along with user-friendly supervisory system. As shown in Fig. 8, a dedicated LabVIEW FPGA program is written in the real-time PXIe-8133 system (FPGA Target) and communicates with an external system. Also, related program for data transferring between LabVIEW and MATLAB generated \*.dll file is deployed in PXI system. Parallel processing is used in the CPU of real-time PXIe-8133 system to meet real-time system criteria. Each loop can be assigned to a dedicated processor and executed in a parallel manner. Fig. 9 shows a part of the interface code which transfers signals from NI 7833R FPGA VI to main processor's code. Based on this issues, generator output signals (i.e., simulated voltages and currents, Fig. 9-A, B) are converted to the real values (Fig. 8-A, B), sent to the analog output FPGA module (Fig. 8-C, D), and then transferred to the real excitation cubicle (Fig. 8-F). In the next step, excitation voltage ( $E_f$ ) from voltage gauges in the excitation system should be returned to NI 7833R FPGA card (Fig. 8-G) through SCB terminal board. The returned signal goes to LabVIEW program as an input (Fig. 9-C) for \*.dll file. Consequently, the loop will be closed to establish the HIL construction. To complete the written program in LabVIEW software, it is necessary to set the analog card so that the received signal being converted precisely (Fig. 8-H). Also, related sampling and preparing output signal codes should be written in FPGA card (Fig. 8-E).

The interaction between MATLAB generated and deployed \*.dll file and real excitation system is executed in the CPU of real-time PXIe-8133 system. MATLAB role is limited to \*.dll file format generation (not PC Windows \*.dll) and after generating an especial library, LabVIEW will use it as an inbuilt function. There is no data exchange between MATLAB and LabVIEW during HIL operation.

In order to change input values for power system analysis and also monitor output data in Fig. 9, LabVIEW graphical pages have been implemented. The operator can change generator, turbine-governor, excitation system, and loads values through human machine interface shown in Fig. 10. The “Generator-

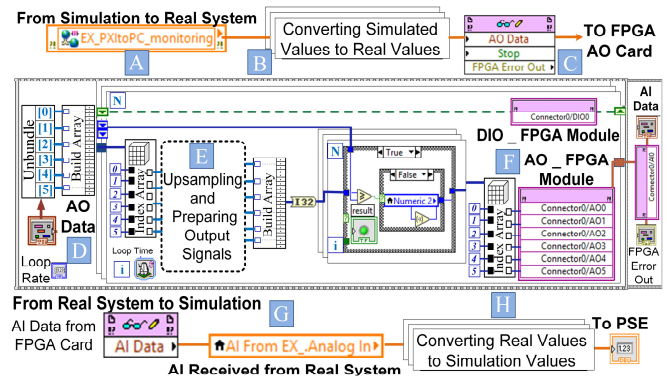


Fig. 8. Dedicated program and related schematic diagram for analog cards in LabVIEW FPGA Module

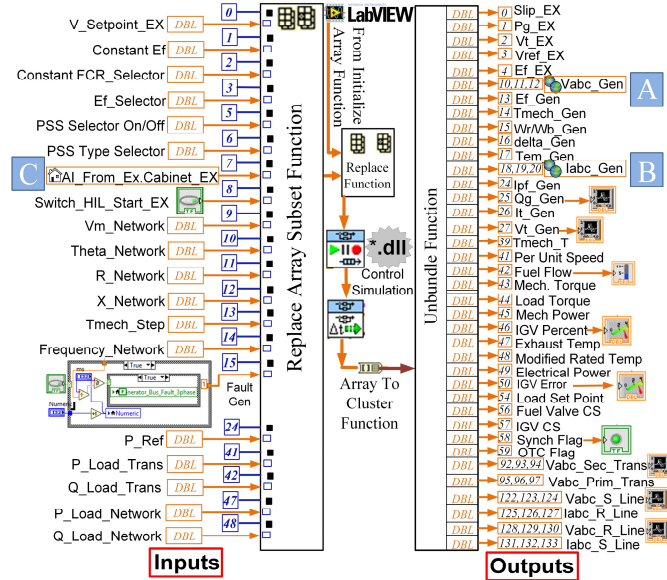


Fig. 9. Data transfer between LabVIEW and MATLAB generated \*.dll file deployed in the PXI real-time system

Bus\_fault” button can simulate fault with predefined fault duration. Also, as magnified in Fig. 10, if the operator clicks on the button named “Switch\_HIL\_Start” in LabVIEW page, the real excitation system will be replaced by the simulated excitation system in MATLAB generated \*.dll file.

There are two parts for monitoring section which are: (1) The parameters related to generator, turbine-governor and excitation system, and (2) the parameters related to transformer, transmission lines, local load, and external grid. As an illustration, the graphical interface created to set the parameters of the generator, turbine-governor and excitation system is shown in Fig. 10.

#### V. EXPERIMENTAL RESULT

##### A. Case Description

In the HIL studies, the real excitation system is connected to the remaining power system model simulated in MATLAB/Simulink and implemented in LabVIEW environment. By pushing the changeover button in LabVIEW graphical environment (Fig. 10), a loop is constructed with the excitation control system working as the hardware (Fig. 6). For validation purposes, experimental results can be compared against the simulation ones in which the real excitation system

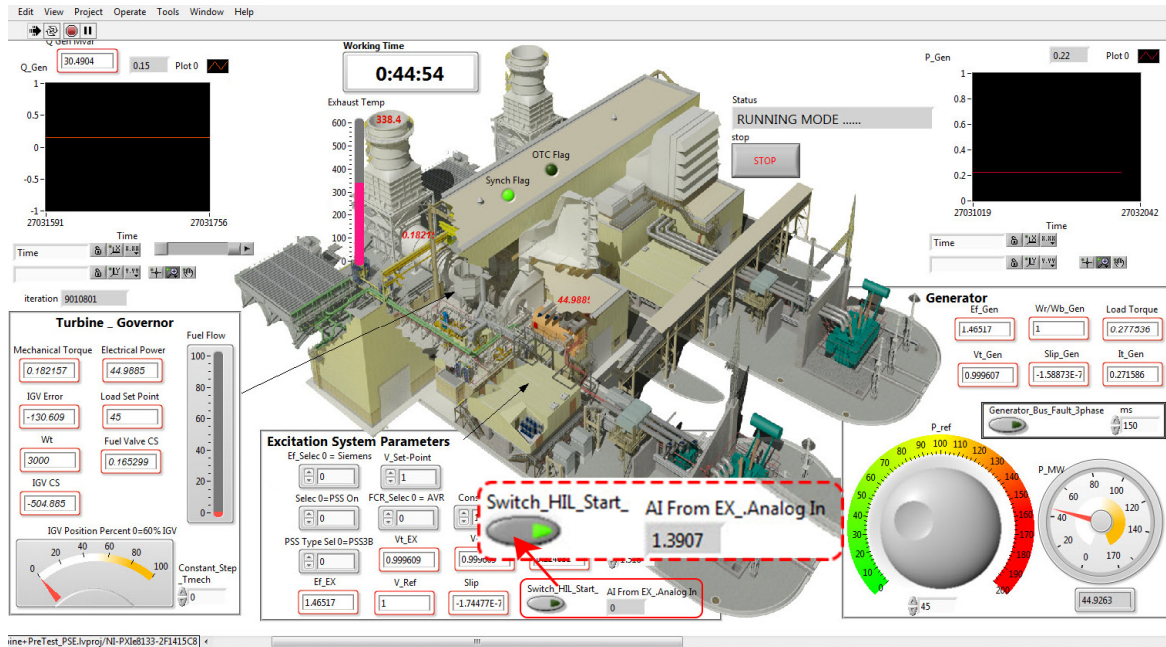


Fig. 10. The parameters related to the generator, turbine-governor and excitation system in LabVIEW page considering changeover switch between two states (real excitation system (HIL) or simulated excitation model)

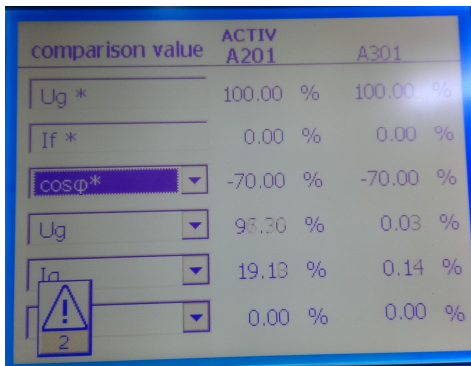


Fig. 11. SIEMENS panel for changing voltage set point.

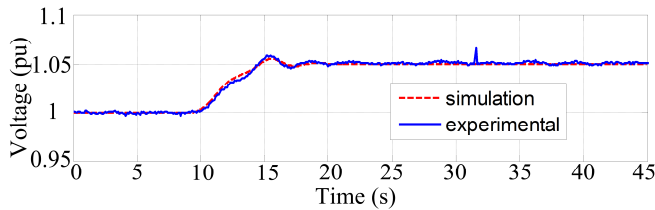


Fig. 12. Simulation and HIL experimental results for the amplitude of synchronous generator output voltage changes after increasing excitation system set point (1 pu to 1.05 pu).

is replaced by its model. HIL system guarantees time precision, less deviation, and fewer jitters.

In the HIL simulations, a 200 MVA 15.75 kV synchronous generator is coupled to a 162.1 MW 3000 rpm steam turbine. A real 1518 kW excitation system from SIEMENS Corporation is connected to the HIL system as shown in Fig. 6. A three-phase transformer and local loads with the active power of 1.5 MW and reactive power of 1 MVAR are also connected to the generator output ( $P_1$  and  $Q_1$  in Fig. 2). Besides, a 32 km transmission line connects the power plant to the infinite bus and loads with the active and reactive powers of respectively 30 MW and 20 MVAR ( $P_2$  and  $Q_2$  in Fig. 2). In these HIL studies,

amplitude, phase angle, and frequency of the infinite bus are 0.95 pu, 0, and 50 Hz, respectively.

Also, it should be added that HIL computation speed is in nature closely relevant to the minimum loop execution time of the hardware under test. Fastest function, in Siemens T400 controller in which almost all of essential exciter related functions is implemented inside, has the loop time of 2 milliseconds (0.5 kHz). This means all digital and analog IOs shall be updated with the rate of 0.5 kHz. In this study and implemented work, minimum calculation time was recorded around 300 microseconds which is more than enough for providing required IOs for the T400 Controller. In each loop, one sample is read from implemented model and sent to the AO card.

In all of the following studies, the time step is 300 microseconds and as the real system (excitation cubicle) time step is 2 milliseconds, no overruns are reported by the system. Also, communication is based on the buffered network shared variables (e.g., voltages, currents, etc.) through 1 gigabit Ethernet and as almost 50 variables each 300 milliseconds shall be sent from target (PXI System with 300 Micro-second loop time) to host (PC Running windows with 300 millisecond loop time), then about  $16\text{bit} * 50 \text{ variables} * 1000 \text{ buffered data} = 800 \text{ K bits}$  of information should be sent every 0.3 second and that's feasible through 1 gigabit Ethernet connection.

### B. Case Studies

As explained previously, a fast, safe, and educational real-time emulator of a complete electric power system is created in which several case studies can be carried out to investigate the effect of various parameters changes of turbine/governor, PSS/AVR, generator, infinite bus, etc., on the whole power system behavior. Different scenarios have been implemented and related results are presented as follows:

#### 1) Generator Voltage Changes

In this case, the interaction between the real excitation and



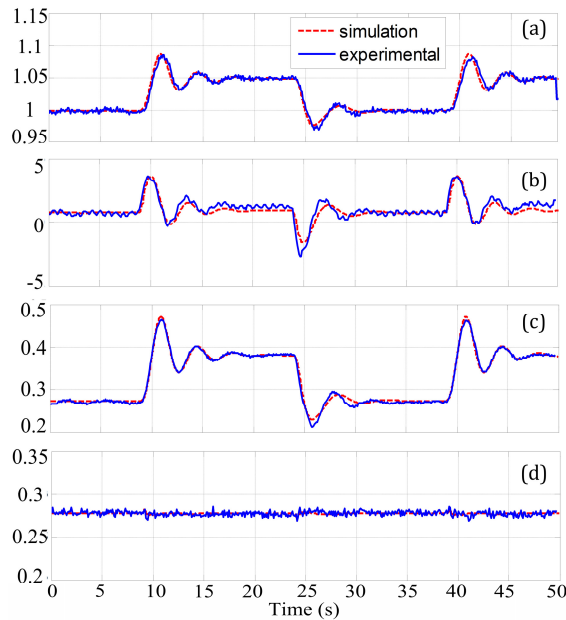


Fig. 13. Comparison between experimental (with the real excitation system working as the hardware in the loop) and simulation results when the reference excitation voltage is changed from 1 to 1.05 pu and vice versa: (a) generator terminal voltage, (b) excitation output voltage, (c) generator output reactive, and (d) active powers.

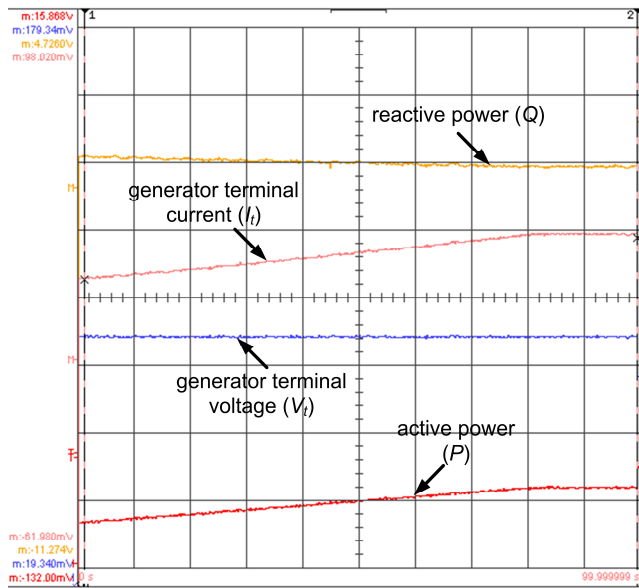


Fig. 14. Oscilloscope traces of synchronous generator output quantities when the after reference active power changes from 45 MW to 85 MW. [Time: 10 s/div,  $V_t$  (stator terminal voltage amplitude): 0.25 pu/div,  $I_i$  (stator terminal current amplitude): 0.25 pu/div,  $P$  (generator active power): 0.25 pu/div, and  $Q$  (generator reactive power): 0.95 pu/div].

the simulated power system is investigated under the changes of the voltage set point of the excitation cubicle (Fig. 11). The voltage set point of the excitation system has been increased from 1 pu to 1.05 pu through SIEMENS panel shown in Fig. 11, while generator is delivering 45 MW to the grid. It should be mentioned that the incremental rate of voltage set point is limited to 0.08 pu/sec which is consistent to the real excitation system settings. This change is applied to MATLAB/Simulink generated \*.dll file (as a LabVIEW inbuilt function) via

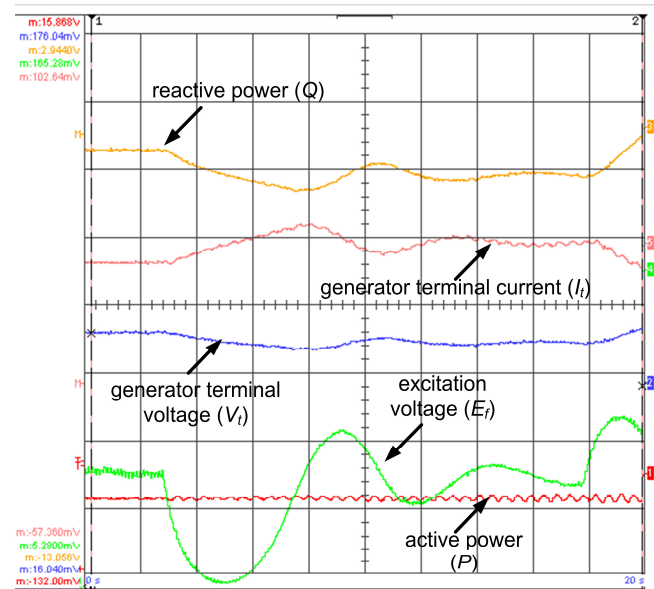


Fig. 15. Oscilloscope traces of synchronous generator output quantities when the under excitation set point changes from 1 pu to 0.95 pu. [Time: 2 s/div,  $V_t$ : 0.25 pu/div,  $I_i$ : 0.25 pu/div,  $P$ : 0.25 pu/div,  $Q$ : 0.95 pu/div, and  $E_f$  (excitation voltage): 0.5 pu/div].

terminal board and PXI system, and then the models respond to this change. Fig. 12 demonstrates the changes in the generator terminal voltage amplitude after increasing excitation system set point. Also, experimental result for this scenario is plotted in the same figure where the real excitation system is replaced by its model. A good matching between the experimental and simulation results is an indicative of the proper settings and modeling of the excitation system.

## 2) Automatic Voltage Regulator (AVR) Step Response

Step response test is one of the important tests in the excitation systems. It shows the accuracy and rapidity of the excitation system in response to the dynamic events. In this case, generator voltage set point ( $V_{t,ref}$ ) has been changed (stepped) and generator terminal and excitation voltages have been monitored. Voltage step changes are implemented directly by T400 SIEMENS board in which excitation system logics are written. Fig. 13 shows the comparison between the simulation and experimental results when the excitation reference voltage is changed stepwise from 1 to 1.05 pu and vice versa. The operating working point is similar to that of the first case study when the change is applied. According to Fig. 13, the generator reactive power changes are similar to those of generator terminal voltage while the active power remains almost constant during the changes. This confirms the fact that the active power is approximately independent of the voltages amplitude.

## 3) Active Power Changes

Active power changes in the power plants are responded by governor fuel valve. In this case, active power changes have been evaluated when the reference active power increases from 45 MW to 85 MW and the results are shown in Fig. 14. It should be mentioned that the active power increment rate is limited to 0.183 MW/sec due to the turbine constraints in normal loading conditions. In the AVR mode, terminal voltage of the generator

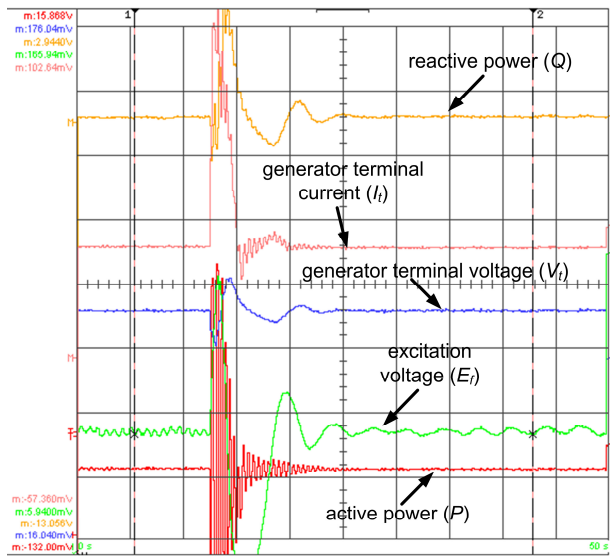


Fig. 16. Oscilloscope traces of synchronous generator output quantities when the electrical frequency of the infinite bus changes from 50 Hz to 49.5 Hz. [Time: 5 s/div,  $V_t$ : 0.25 pu/div,  $I_t$ : 0.25 pu/div,  $P$ : 0.25 pu/div,  $Q$ : 0.95 pu/div, and  $E_f$ : 0.5 pu/div].

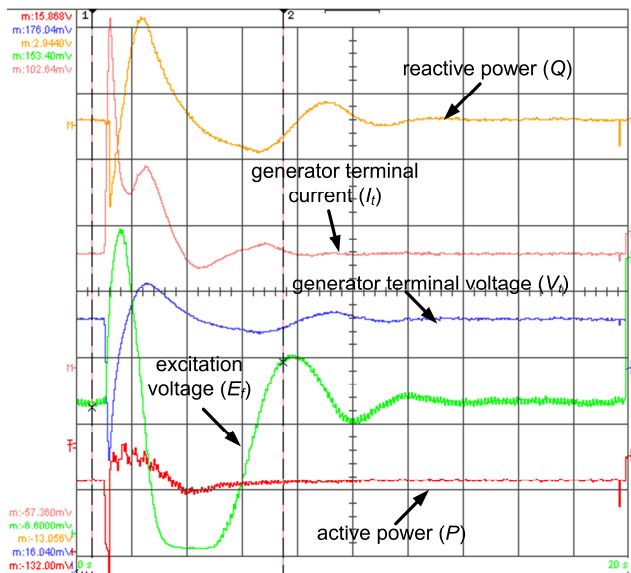


Fig. 17. Oscilloscope traces of synchronous generator output quantities when a three-phase fault occurs at the generator terminals and then removed after 150 ms. [Time: 2 s/div,  $V_t$ : 0.25 pu/div,  $I_t$ : 0.25 pu/div,  $P$ : 0.25 pu/div,  $Q$ : 0.95 pu/div, and  $E_f$ : 0.5 pu/div].

is kept constant at 1 pu by the excitation system during the active power changes.

#### 4) Under Excitation Test

If reactive power decreases to values less than its minimum margin, the generator will go into instability. Continuing with the generator bus voltages decrement, excitation system reacts and tries to increase excitation voltage and; consequently, reactive power generation will increase. This scenario has been implemented and the minimum margin is changed by the operator in order to meet the under excitation limit. It should be noted that generator voltage is given to the Siemens Exciter by user or DCS, if the set point is less than the generator terminal

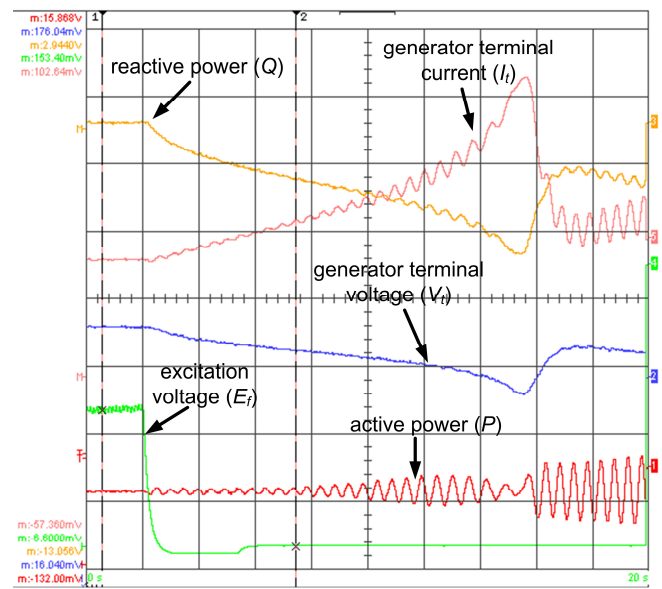


Fig. 18. Oscilloscope traces of synchronous generator output quantities after disconnection of real excitation system. [Time: 2 s/div,  $V_t$ : 0.25 pu/div,  $I_t$ : 0.25 pu/div,  $P$ : 0.25 pu/div,  $Q$ : 0.95 pu/div, and  $E_f$ : 0.5 pu/div].

voltage, negative reactive power will be the outcome. If the user persists in decreasing the set point, the possibility of under excitation and instability occurrence will increase.

To simulate this situation and monitor under excitation limitation in the test field, under excitation set point has been changed from 1 pu to 0.95 pu in T400 software while the generator is delivering 81 MW to the grid. Fig. 15 confirms the above explanations. As shown in this figure, the excitation system increases the generator terminal voltage when a violation of the reactive power below its minimum margin is sensed. Consequently, depending on active power value and grid voltage, stator voltage is increased automatically by the excitation system preventing the machine instability.

#### 5) Electrical Frequency Change

Electrical frequency can be changed in the PSE system through LabVIEW real-time software. By changing the electrical frequency, the active power will change (droop mode). In this scenario, the electrical frequency of the infinite bus has been changed in PSE page from 50 Hz to 49.5 Hz when the generator output power is 81 MW and its terminal voltage is set to 1 pu by the excitation system. Fig. 16 shows that 1% of speed drop concludes to the increment of generator output active power from 81 MW to 81.9 MW.

#### 6) Generator three-phase fault

Through the three-phase switch provided in the MATLAB/Simulink file for three-phase fault studies (Fig. 2), operator can simulate generator terminal three-phase short-circuit in PSE and investigate the response of the real excitation system and its control with no risk of damage to the generator. During the test, while real excitation system maintains the generator output voltage at 1 pu and the generator output power is 81 MW, a three-phase fault with specified duration, e.g., 150 ms, is exerted by generator bus voltage button. According to Fig. 17, generator voltage is zero during the short circuit and as

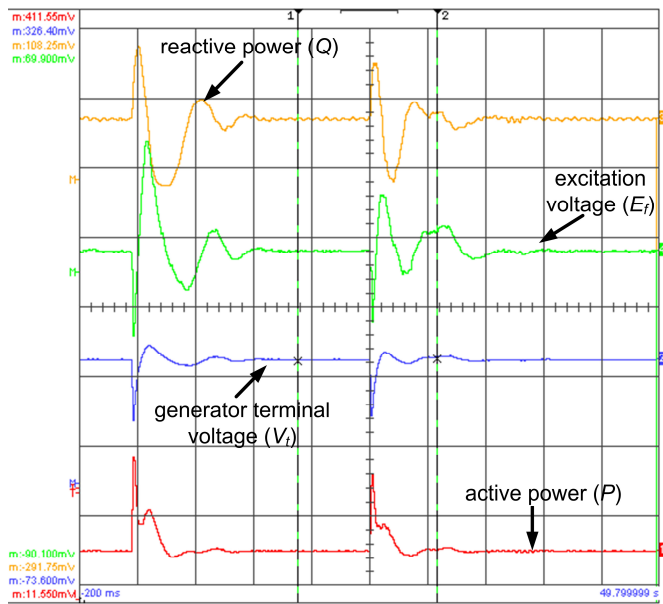


Fig. 19. Oscilloscope traces of synchronous generator output quantities for PSS is OFF and then ON when a disturbance is applied. [Time: 2 s/div,  $V_t$ : 0.25 pu/div,  $P$ : 0.25 pu/div,  $Q$ : 0.95 pu/div, and  $E_f$ : 0.5 pu/div].

AVR tries to increase the terminal voltage, a huge voltage spike from excitation can be observed. There is also a sudden decrease of reactive power as a consequence of short-circuit; then, it faces a sudden increase as the generator terminal voltage is increased due to the function of excitation system.

#### 7) Instability analysis after disconnection of excitation system

In real systems, if excitation circuit is disconnected, generator protection system will act and consequently grid circuit breaker (GCB) will be opened. In PSE simulation system, operator can simulate this scenario by disconnecting the real excitation system from the NI-SCB-68 board and see what happens if there is no disconnection from the grid (consider GCB is not acting or basically there is no GCB). Fig. 18 shows that generator terminal voltage will step down due to the removal of rotor electromagnetic field. As a result, reverse power procedure is triggered. Interestingly, as the turbine is coupled with rotor and is rotating in synchronous speed, rotor induced flux from reverse power phenomenon will lead to a steep jump of reactive power. This chain of events will continue as long as GCB remains closed.

#### 8) PSS Test

The effects of PSS in damping the disturbances can be investigated through PSE simulator. As shown in Fig. 19, a disturbance is exerted on the system at  $t = 5$  s while the PSS is OFF and the same disturbance is applied at  $t = 25$  s in which the PSS is activated. The differences between two cases (PSS ON and PSS OFF) after event occurrence clarify that in PSS ON mode, the disturbance will damp faster than another mode.

## VI. CONCLUSION

In this paper we implemented HIL system with a real excitation cubicle related to electrical power systems. Based on this issue, power network components have been modeled in

MATLAB. LabVIEW and related hardware were used to complete the close loop between MATLAB/Simulink models, i.e. \*.dll generated file, and excitation cubicle demonstrating the efficacy and applications of HIL real-time simulation in the power system industry. Good matching between the real-time emulated system and offline simulation results confirm the effectiveness of the proposed Power System Emulator (PSE). Such a real-time emulator of the power system can be used in order to test new controller and related devices before installation in the real power plant. Compared to other test approaches, it is a low-cost solution since the whole power plant except, the under test device, can be simulated in MATLAB/Simulink with a high capability in debugging mode.

following conclusion can be drawn from the present study:

1) Outstanding features of LabVIEW and related NI PXI hardware have been presented. The graphical user interface to the experimental procedure and fast time cycle can perform many studies in power system analysis.

2) PSE helps operators in power plants to perform complex experiments in a safe manner. In this case, as a training simulator, they can also perform different scenarios without any risk and learn how to react in critical conditions. Different real events can be implemented in PSE in order to assess power system reaction.

3) In this paper, the proposed PSE provides a versatile and fast solution for testing excitation system in critical scenarios. Consistent to this matter, capability of excitation system under different conditions (generator three-phase fault, electrical frequency/active power change, generator voltage changes, voltage step response, etc.) can be determined at the test field in the factory and its drawbacks can be fixed before commercializing of product and without the risk of damaging the actual electric power equipment.

4) Compared to commercial simulators in the market such as Opal-RT, dSPACE, RT-Box or Typhoon HIL which are expensive, PSE simulator is low-cost and economical. Also, most of the existing simulators are designed for end user and do not support new equipment modeling, implementing modification or development. Consistent to this issue, user is forced to use simulator's library and employ the provided hardware. On the contrary, PSE simulator has a flexible and expandable structure which uses general hardware and software from National Instrument company linked to MATLAB through \*.dll generated file as a LabVIEW inbuilt function. This versatile simulator allows everyone to set up his own desired hardware with much lower price achieved by omitting unnecessary hardware and software modules in the pre-built simulators.

## Acknowledgement

This work was supported by the MAPNA Electrical and Control Engineering and Manufacturing Company (MECO). The authors would like to express sincere appreciation for company's funding on this research.





**Ali Parizad** (SM' 2008, GSM' 2011) received his M.S. in Electrical Engineering from Iran University of Science and Technology (IUST) in 2010. He joined MAPNA Electric and Control Eng. and Manuf. Co. (MECO) in 2010 as power systems analysis expert. He was an EMS and SCADA expert as well as commissioning supervisor in many Substations and Power Plants with ABB and SIEMENS

Companies. He has been participated in different projects in fields of power plants, SCADA and Railway systems. He has also done several projects in the field of real-time simulators and registered a patent on real-time islanded simulator for industrial power plants. He is author of two published book chapters, three books, and 22 conference and journal papers. His special fields of interest are smart grids, distributed generation and renewable energies, power system operation and control, and application of real-time simulator in the power systems.



**Sobhan Mohamadian** received his B.Sc. and Ph.D. degrees in Electrical Engineering from Iran University of Science and Technology (IUST), Tehran, Iran, in 2007 and 2016, respectively.

Between February 2014 and March 2015, he spent a period as a visiting scholar at the University of Trieste, Trieste, Italy, where he worked on research projects regarding high-power multiphase motor drives and multiphase machine modeling and analysis. In 2016 he joined the University of Damghan, Damghan, Iran, where he is currently working as an assistant professor.

His current research interests include power quality, power electronics and electrical machines modeling and drives.



**Mohamad Esmail Iranian** received his B.Sc. degree in power engineering from Tehran-South Azad University, Tehran, Iran in 2005. From 2005 to 2007 he was engaged with tele-control projects in Neda Corps. In 2008 he joined MAPNA-MECO commissioning team for Siemens and ABB Static Exciters and Static MEGA Drives. He was a commissioning supervisor in many Power Plants with either ABB

or SIEMENS S.E.Es or S.F.Cs. From 2010 to 2018, he was engaged with R&D Department of MECO and he has been participated in different power electronic projects in field of renewable energy & Gas and steam Exciters. He has also done several projects in the field of Power System HIL Emulators and holds an Iranian patent on Hardware in Loop RT Emulator for P.P Exciters.



**Josep M. Guerrero** (S'01-M'04-SM'08-FM'15) received the B.S. degree in telecommunications engineering, the M.S. degree in electronics engineering, and the Ph.D. degree in power electronics from the Technical University of Catalonia, Barcelona, in 1997, 2000 and 2003, respectively. Since 2011, he has been a Full Professor with the Department of Energy

Technology, Aalborg University, Denmark, where he is responsible for the Microgrid Research Program ([www.microgrids.et.aau.dk](http://www.microgrids.et.aau.dk)). From 2012 he is a guest Professor at the Chinese Academy of Science

and the Nanjing University of Aeronautics and Astronautics; from 2014 he is chair Professor in Shandong University; from 2015 he is a distinguished guest Professor in Hunan University; and from 2016 he is a visiting professor fellow at Aston University, UK, and a guest Professor at the Nanjing University of Posts and Telecommunications. His research interests is oriented to different microgrid aspects, including power electronics, distributed energy-storage systems, hierarchical and cooperative control, energy management systems, smart metering and the internet of things for AC/DC microgrid clusters and islanded minigrids; recently specially focused on maritime microgrids for electrical ships, vessels, ferries and seaports. Prof. Guerrero is an Associate Editor for a number of IEEE TRANSACTIONS. He received the best paper award of the IEEE Transactions on Energy Conversion for the period 2014-2015, and the best paper prize of IEEE-PES in 2015. As well, he received the best paper award of the Journal of Power Electronics in 2016. In 2014, 2015, 2016, and 2017 he was awarded by Thomson Reuters as Highly Cited Researcher, and in 2015 he was elevated as IEEE Fellow for his contributions on "distributed power systems and microgrids."

## References

- [1] S. Mohamadian, A. Tassarolo, S. Castellan, and A. Shoulaie, "Steady-state simulation of LCI-fed synchronous motor drives through a computationally-efficient algebraic method," *IEEE Trans. Power Electron.*, vol. 32, no. 1, pp. 452-470, Jan. 2017.
- [2] S. Mohamadian, S. Castellan, A. Tassarolo, G. Ferrari, and A. Shoulaie, "An algebraic algorithm for motor voltage waveform prediction in dual-LCI drives with interconnected DC-links," *IEEE Trans. Energy Convers.*, vol. 31, no. 2, pp. 506-519, Jun. 2016.
- [3] Y. V. P. Kumar and R. Bhimasingu, "Alternative hardware-in-the-loop (HIL) setups for real-time simulation and testing of microgrids," *2016 IEEE 1st International Conference on Power Electronics, Intelligent Control and Energy Systems (ICPEICES)*, Delhi, India, 2016, pp. 1-6.
- [4] V. R. Dinavahi, M. Reza Iravani and R. Bonert, "Real-time digital simulation of power electronic apparatus interfaced with digital controllers," *IEEE Trans. Power Del.*, vol. 16, no. 4, pp. 775-781, 2001.
- [5] O. Goñi, A. Sanchez, E. Todorovich, and A. de Castro, "Resolution analysis of switching converter models for hardware-in-the-loop," *IEEE Trans. Ind. Informat.*, vol. 10, no. 2, pp. 1162-1170, May 2014.
- [6] Ó. Lucia, I. Urriza, L. A. Barragan, D. Navarro, Ó. Jimenez, and J. M. Burdio, "Real-time FPGA-based hardware-in-the-loop simulation test bench applied to multiple-output power converters," *IEEE Trans. Ind. Appl.*, vol. 47, no. 2, pp. 853-860, Mar./Apr. 2011.
- [7] M. O. Omar Faruque and V. Dinavahi, "Hardware-in-the-loop simulation of power electronic systems using adaptive discretization," *IEEE Trans. Ind. Electron.*, vol. 57, no. 4, pp. 1146-1158, Apr. 2010.
- [8] M. Dagbagi, A. Hemdani, L. Idkhajine, M. W. Naouar, E. Monmasson, and I. Slama-Belkhdja, "ADC-based embedded real-time simulator of a power converter implemented in a low-cost FPGA: application to a fault-tolerant control of a grid-connected voltage-source rectifier," *IEEE Trans. Ind. Electron.*, vol. 63, no. 2, pp. 1179-1190, Feb. 2016.
- [9] W. Wang, Z. Shen and V. Dinavahi, "Physics-based device-level power electronic circuit hardware emulation on FPGA," *IEEE Trans. Ind. Informat.*, vol. 10, no. 4, pp. 2166-2179, Nov. 2014.
- [10] J. Liu and V. Dinavahi, "Detailed magnetic equivalent circuit based real-time nonlinear power transformer model on FPGA for electromagnetic transient studies," *IEEE Trans. Ind. Electron.*, vol. 63, no. 2, pp.1191-1202, Feb. 2016.
- [11] F. R. Palomo Pinto and A. P. Vega-Leal, "A test of HIL COTS technology for fuel cell systems emulation," *IEEE Trans. Ind. Electron.*, vol. 57, no. 4, pp. 1237-1244, Apr. 2010.
- [12] L. Bun, B. Raison, G. Rostaing, S. Bacha, A. Rumeau, and A. Labonne "Development of a real time photovoltaic simulator in normal and abnormal operations," in *Proc. 37th Annu. IEEE IECON*, Melbourne, Australia, Nov. 7-10, 2011, pp. 867-872.
- [13] S. J. Pinto, G. Panda, and R. Peesapati, "An implementation of hybrid control strategy for distributed generation system interface using Xilinx system generator," *IEEE Trans. Ind. Informat.*, vol. 13, no. 5, pp. 2735-2745, Oct. 2017.



- [14] Q. Shafiee, T. Dragičević, J. C. Vasquez, and J. M. Guerrero, "Hierarchical control for multiple DC-microgrids clusters," *IEEE Trans. Energy Convers.*, vol. 29, no. 4, pp. 922-933, Dec. 2014.
- [15] R. Gagnon *et al.*, "Large-scale real-time simulation of wind power plants into Hydro-Québec power system," in *Proc. 9th Wind Integr. Workshop*, Quebec City, QC, Canada, Oct. 18-19, 2010, pp. 73-80.
- [16] I. Munteanu, A. I. Bratcu, S. Bacha, D. Roye, and J. Guiraud, "Hardware in-the-loop-based simulator for a class of variable-speed wind energy conversion systems: Design and performance assessment," *IEEE Trans. Energy Convers.*, vol. 25, no. 2, pp. 564-576, Jun. 2010.
- [17] G. F. Lauss, M. O. Faruque, K. Schoder, C. Dufour, A. Viehweider, and J. Langston, "Characteristics and design of power hardware-in-the-loop simulations for electrical power systems," *IEEE Trans. Ind. Electron.*, vol. 63, no. 1, pp. 406-417, Jan. 2016.
- [18] A. Helmedag, T. Isermann, and A. Monti, "Fault ride through certification of wind turbines based on a hardware in the loop setup," *IEEE Trans. Instrum. Meas.*, vol. 63, no. 10, pp. 2312-2321, Oct. 2014.
- [19] M. Steurer, C. S. Edrington, M. Sloderbeck, W. Ren, and J. Langston, "A megawatt-scale power hardware-in-the-loop simulation setup for motor drives," *IEEE Trans. Ind. Electron.*, vol. 57, no. 4, pp. 1254-1260, Apr. 2010.
- [20] W. Ren, M. Steurer, and T. L. Baldwin, "An effective method for evaluating the accuracy of power hardware-in-the-loop simulations," *IEEE Trans. Ind. Appl.*, vol. 45, no. 4, pp. 1484-1490, Jul./Aug. 2009.
- [21] C. Dufour and J. Bélanger, "On the use of real-time simulation technology in smart grid research and development," *IEEE Trans. Ind. Appl.*, vol. 50, no. 6, pp. 3963-3970, Nov./Dec. 2014.
- [22] W. Ren, M. Steurer, and T. L. Baldwin, "Improve the stability and the accuracy of power hardware-in-the-loop simulation by selecting appropriate interface algorithms," *IEEE Trans. Ind. Appl.*, vol. 44, no. 4, pp. 1286-1294, Jul./Aug. 2008.
- [23] J. Rodríguez-Reséndiz, G. Herrera-Ruiz, and E. A. Rivas-Araiza, "Adjustable speed drive project for teaching a servo systems course laboratory," *IEEE Trans. Educ.*, vol. 54, no. 4, pp. 657-666, Nov. 2011.
- [24] J. M. Jiménez-Martínez, F. Soto, E. de Jódar, J. A. Villarejo, and J. Roca-Dorda, "A new approach for teaching power electronics converter experiments," *IEEE Trans. Educ.*, vol. 48, no. 3, pp. 513-519, 2005.
- [25] M. A. Stegawski and R. Schaumann, "A new virtual-instrumentation-based experimenting environment for undergraduate laboratories with application in research and manufacturing," *IEEE Trans. Instrum. Meas.*, vol. 47, no. 6, pp. 1503-1506, Dec. 1998.
- [26] F. Adamo, F. Attivissimo, G. Cavone, and N. Giaquinto, "SCADA/HMI systems in advanced educational courses," *IEEE Trans. Instrum. Meas.*, vol. 56, no. 1, pp. 4-10, Feb. 2007.
- [27] J. Pantelic-Babic, V. Jankovic, and P. Bosnjakovic, "System for electromotive force standards comparison based on virtual instrument," *IEEE Trans. Instrum. Meas.*, vol. 51, no. 6, pp. 1295-1299, Dec. 2002.
- [28] S. Caldara, S. Nuccio, and C. Spataro, "A virtual instrument for measurement of flicker," *IEEE Trans. Instrum. Meas.*, vol. 47, no. 5, pp. 1155-1158, Oct. 1998.
- [29] T. Orłowska-Kowalska and M. Kaminski, "FPGA implementation of the multilayer neural network for the speed estimation of the two-mass drive system," *IEEE Trans. Ind. Informat.*, vol. 7, no. 3, pp. 436-445, Aug. 2011.
- [30] J. Wang, Y. Song, W. Li, J. Guo, and A. Monti, "Development of a universal platform for hardware in-the-loop testing of microgrids," *IEEE Trans. Ind. Informat.*, vol. 10, no. 4, pp. 2154-2165, Nov. 2014.
- [31] A. S. Musleh, S. M. Muyeen, A. Al-Durra, I. Kamwa, M. A. S. Masoum, and S. Islam, "Time-delay analysis of wide area voltage control considering smart grid contingences in real-time environment" *IEEE Trans. Ind. Informat.*, vol. 14, no. 3, pp. 1242-1252, Mar. 2018.
- [32] W. Winiński, "Methodology of virtual instrument time analysis," *IEEE Trans. Instrum. Meas.*, vol. 55, no. 1, pp. 21-25, Feb. 2006.
- [33] P. Bilski and W. Winiński, "Time optimization of soft real-time virtual instrument design," *IEEE Trans. Instrum. Meas.*, vol. 54, no. 4, pp. 1412-1416, Aug. 2005.
- [34] H. M. G. Ramos, J. M. Dias Pereira, V. Viegas, O. Postolache, and P. M. B. Silva Girão, "A virtual instrument to test smart transducer interface modules (STIMs)," *IEEE Trans. Instrum. Meas.*, vol. 53, no. 4, pp. 1232-1239, Aug. 2004.
- [35] C. A. Cansalar, E. Maviş and C. Kasnakoğlu, "Simulation time analysis of MATLAB/Simulink and LabVIEW for control applications," *2015 IEEE International Conference on Industrial Technology (ICIT)*, Seville, 2015, pp. 470-473.
- [36] C.-M. Ong, *Dynamic Simulation of Electric Machinery Using Matlab/Simulink*. Englewood Cliffs, NJ: Prentice-Hall, 1999.
- [37] P. C. Krause, *Analysis of Electrical Machinery.*, McGraw-Hill, 1987.
- [38] W. I. Rowen, "Simplified mathematical representations of single shaft gas turbines in mechanical drive service," in *Proc. Int. Gas Turbine and Aeroengine Congr. and Expo.*, Cologne, Germany, 1992.
- [39] L. M. Hajagos and G. R. Berube, "Utility experience with gas turbine testing and modeling," in *Proc. Power Engineering Society Winter Meeting*, Columbus, OH, Jan. 28-Feb. 1, 2001, vol. 1.
- [40] M. Nagpal, A. Moshref, G. K. Morison, and P. Kundur, "Experience with testing and modeling of gas turbines," in *Proc. IEEE Power Engineering Society General Meeting*, Columbus, OH, Jan. 28-Feb. 1, 2001, vol. 2.
- [41] L. N. Hannett and A. H. Khan, "Combustion turbine dynamic model validation from tests," *IEEE Trans. Power Syst.*, vol. 8, no. 1, pp. 152-158, Feb. 1993.
- [42] National Instrument Corp, [Online]. Available: <http://www.ni.com>
- [43] [www.ni.com/pdf/manuals/372870d.pdf](http://www.ni.com/pdf/manuals/372870d.pdf).
- [44] M. E. Iranian, A. Zabihi nejad "Modeling and implementation of generator and network simulator for static exciters using MATLAB and LabVIEW" *Journal of Applied Sciences*, doi:10.3923/jas.2011.
- [45] M. E. Iranian, I. Yousefi, M. Aliyari "Real-time dynamic HIL simulator of gas turbine, governor, generator and grid for static excitation of a 200-MVA synchronous generator" *Journal of SIMULATION*, vol. 90, no. 10, pp. 1129-1145, Oct. 2014.